Available online at www.pelagiaresearchlibrary.com

Pelagia Research Library

Pelagia Research Library

Advances in Applied Science Research, 2016, 7(3):45-57

Advances in Applied Science Research
Pelagia Research Library
ISSN: 0976-8610
CODEN (USA): AASRFC

Determining the potential field within a square transformer

Ouigou M. Zongo[1], Sié Kam[2], Tassembedo Sosthène[2], Kounhinir Some[1], Kalifa Palm[3] and Alioune Ouedraogo[2]

[1]*Département de Mathématiques, UFR-SEA, Université de Ouagadougou, B.P 7021, Ouagadougou 03, Burkina Faso*
[2]*Département de Physique, UFR-SEA, Université de Ouagadougou, B.P 7021, Ouagadougou 03, Burkina Faso*
[3]*Institut de Recherche en Sciences Appliquées et Technologies 03 BP 7047 Ouagadougou 03, Burkina Faso*

ABSTRACT

This paper deals with determining a field of stationary potential in a transformer with square plane section, with a side measuring 4 and divided at the center by a square which side measures 2. The problem consists in solving a Laplace equation with conditions on Dirichlet's boundaries that we solve using the method of large singular finite elements method (LSFEM). Then, we compare the values of the solution u *and those of its first derivatives with those obtained using the finite element method (FEM). Both methods provide results that align everywhere except near singularities where there are very significant gaps.*

Keywords: potential field, large elements, finite elements, singularities.

INTRODUCTION

The Laplace's equation and more generally, the Poisson's equation is used to solve several engineering problems and in other subjects. This equation is used in electromagnetism [1], heat transmission [2], fluid dynamics [3], elasticity [4-5] and in potential theory [6]. When the problem is singular to the polygon summits, the numerical solving of the Laplace's equation is very difficult and usual finite element methods do not provide satisfactory results when they are used in their standard form. These methods as shown by various authors [7-16] may be slightly improved if they take the analytical form of the solution near the singularities into account. We use LSFEM to determine the potential field in a square transformer with Dirichlet's non-homogenous boundary conditions. This gives good results in the entire domain studied while FEM gives good results only in areas that are far from singularities. This shows the power, efficiency, and accuracy of this method with a limited number of coefficients compared to finite element method.

MATERIALS AND METHODS

Let's determine the potential stationary field within the square transformer which side is 4, cut in its center by a square which side is 2. We assume that the variables have been reduced by modifying the scale (adimensioning). The reduced potential $u(x, y)$ is 1 on the contour $\partial\Omega_2$ of the internal square and 0 on the external border $\partial\Omega_1$ of the domain Ω while between two squares, it should confirm the Laplace's equation (figure 1).

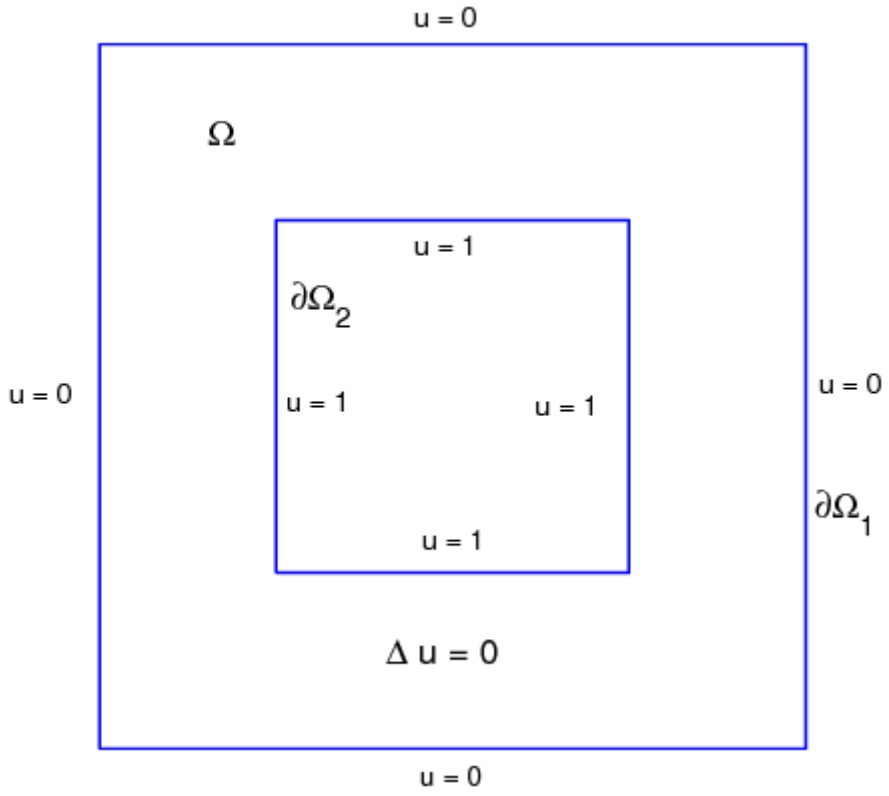

Figure 1: Domain of the Square Transformer

Though the initial domain is pierced and that limit conditions are Dirichlet-like, we may, because of elements like the double geometrical symmetric of the domain, the conditions on limits and the Laplace's operator, work on the one eighth of the transformer. The domain then considered is a rectangular trapezium ACDE (figure 2). The problem will then consist in solving the Laplace's equation on the polygonal domain ACDE with mixed limit conditions:

$\Delta u(x, y) = 0$ within the trapezoid domain ACDE (1)

$u(x, y) = 0$ along AC (2)

$u(x, y) = 1$ along DE (3)

$\frac{\partial u}{\partial n} = 0$ along AE (4)

$\frac{\partial u}{\partial n} = 0$ along CD (5)

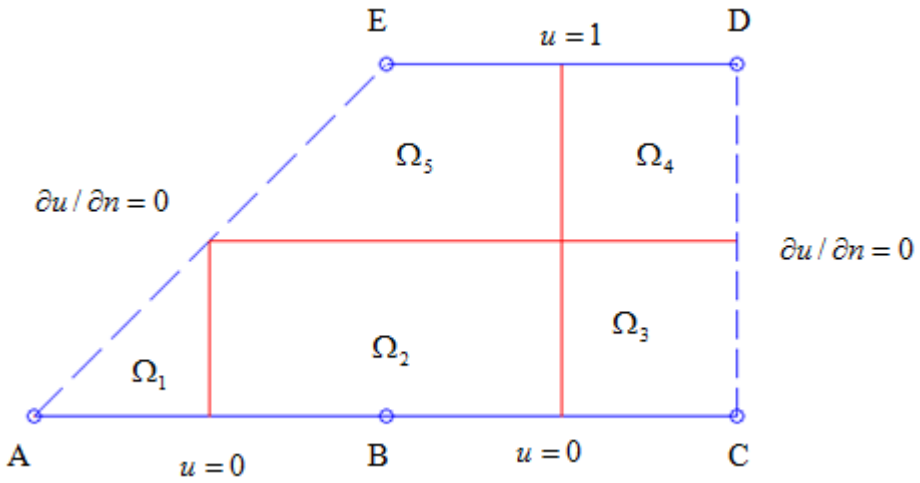

Figure 2 : The eighth of the square transformer is dived into five subdomains

The problem as posed is particular because of the geometrical singularities that are the vertices of the polygon domain where there is a sudden change in the direction of the normal at the boundary. Neumann's homogenous limit conditions have been imposed on sides AE and CD and Dirichlet's ones are used on sides AC and DE. Let's solve it using the method of large singular finite elements that includes three steps:

Step1 : Dividing the domain

The figure 2 shows the division of the domain ACDE into five sub-domains bearing five singularities as recommended by Tolley [9] and condition to Neumann-Dirichlet mixed limits. The border of the working domain has been drawn in blue, the continuous lines show the parts of the border on which conditions to limits are Dirichlet-like while discontinuous lines are conditions to Neumann's limits. Sub-borders Γ_{ij} that separate subdomains Ω_i and Ω_j are in red.

Step 2: Solving auxiliary problems

To each subdomain Ω_i, $i=1,..,5$ is given a system of local coordinates and problem. For the subdomain Ω_5, which extension is Ω_5^*, the system of polar coordinate (r_5,θ_5) and the conditions to limits are summarized in figure 3 below.

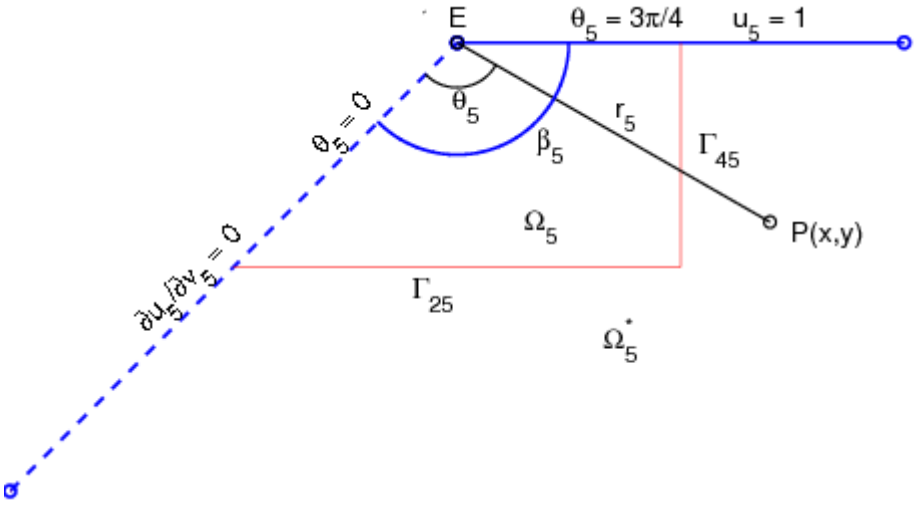

Figure 3 : The subdomain Ω_5, its opening β_5 and its local coordinates (r_5,θ_5).

We must solve the following five auxiliary problems on Ω_i:

First auxiliary problem

$$u_1(r_1,\theta_1)=0 \quad (r_1,\theta_1)\in\Omega_1^* \tag{6}$$

$$u_1(r_1,0)=0 \tag{7}$$

$$u_1(r_1,\frac{\pi}{4})=0 \tag{8}$$

Second auxiliary problem

$$u_2(r_2,\theta_2)=0 \quad (r_2,\theta_2)\in\Omega_2^* \tag{9}$$

$$u_2(r_2,0)=0 \tag{10}$$

$$u_2(r_2,\pi)=0 \tag{11}$$

Third auxiliary problem

$$\Delta u_3(r_3,\theta_3)=0 \quad (r_3,\theta_3)\in\Omega_3^* \tag{12}$$

$$u_3(r_3,0)=0 \tag{13}$$

$$u_3(r_3,\frac{\pi}{2})=0 \tag{14}$$

Fourth auxiliary problem

$$\Delta u_4(r_4,\theta_4)=0 \qquad (r_4,\theta_4)\in \Omega_4^* \tag{15}$$

$$u_4(r_4,0)=1 \tag{16}$$

$$u_4(r_4,\frac{\pi}{2})=0 \tag{17}$$

Fifth auxiliary problem

$$\Delta u_5(r_5,\theta_5)=0 \qquad (r_5,\theta_5)\in \Omega_5^* \tag{18}$$

$$\frac{\partial u_5(r_5,0)}{\partial n_5}=0 \tag{19}$$

$$u_5(r_5,\frac{3\pi}{4})=0 \tag{20}$$

All general solutions to auxiliary problems are not alike, they depend on the opening of the angle β_i and conditions to limits [8,9] are written as follow:

$$u_1(r_1,\theta_1)=\sum_{i=1}^{\infty} a_{1i} r_1^{2i-1}\sin(2i-1)\theta_1 \tag{21}$$

$$u_2(r_2,\theta_2)=\sum_{j=1}^{\infty} a_{2j} r_2^{2j}\sin(2j\theta_2) \tag{22}$$

$$u_3(r_3,\theta_3)=\sum_{k=1}^{\infty} a_{3k} r_3^{2k-1}\cos(2k-1)\theta_3 \tag{23}$$

$$u_4(r_4,\theta_4)=1+\sum_{l=1}^{\infty} a_{4l} r_4^{2l-1}\sin(2l-1)\theta_4 \tag{24}$$

$$u_5(r_5,\theta_5)=1+\sum_{m=1}^{\infty} a_{5m} r_5^{\frac{(4m-2)}{3}}\sin\frac{4m-2}{3}\theta_5 \tag{25}$$

with coefficients $a_{1i,}$ $a_{2j,}$ a_{3k}, a_{4l} and a_{5m} arbitrary constants.

Practically, we must keep to approximate solutions. The approximation derives, on the one hand, from the fact that there is a need to limit developments (21) to (25) to a finite number of terms and, on the other hand, we must keep, except few cases, to an imperfect alignment. The number of coefficients kept in each of the sums has been chosen according to Descloux and Tolley's [9, 13] principle, which aims at representing approximate solutions using uniforms function as possible. This ensures an overall homogeneity to the approximate solutions obtained while keeping more terms for subdomains where openings are larger. We decide to keep a number of coefficients proportional to the angle $\beta_k,(k=1,\ldots,5)$, with the opening extension Ω_k^* of the subdomain Ω_k.

$$u_1(r_1,\theta_1)=\sum_{i=1}^{N} a_{1i} r_1^{2i-1}\sin(2i-1)\theta_1 \tag{26}$$

$$u_2(r_2,\theta_2)=\sum_{j=1}^{4N} a_{2j} r_2^{2j}\sin(2j\theta_2) \tag{27}$$

$$u_3(r_3,\theta_3)=\sum_{k=1}^{2N} a_{3k} r_1^{2k-1}\cos(2k-1)\theta_3 \tag{28}$$

$$u_4(r_4,\theta_4) = 1 + \sum_{l=1}^{2N} a_{4l} r_4^{2l-1} \sin(2l-1)\theta_4 \quad (29)$$

$$u_5(r_5,\theta_5) = 1 + \sum_{m=1}^{3N} a_{5m} r_5^{\frac{(4m-2)}{3}} \sin(\frac{4m-2}{3})\theta_5 \quad (30)$$

The total number of coefficients a_{kl} which value may be freely selected will be

(1+4+2+2+3) N = 12N where N is the number of coefficients kept for an opening angle $\pi/4$.

Step 3: Aligning auxiliary solutions

To get the solution of the initial problem (1) to (3) from solutions to auxiliary problems, we "just" need to make "a good choice" of arbitrary coefficients a_{in}. According to M. D. Tolley [9], the relevant choice is made by setting the continuity of auxiliary functions and those of their normal derivatives. We are aligning the solutions of the auxiliary problems to the meaning of the continuous least squares, or we have been determining the coefficients a_{kl} that allow minimizing the function:

$$I(a_{mn}) = \sum_{i<j} \int_{\Gamma_{ij}} \left[(u_i(a_{ik}) - u_j(a_{jl}))^2 + \left(\frac{\partial u_i(a_{ik})}{\partial n_i} + \frac{\partial u_j(a_{jl})}{\partial n_j} \right)^2 \right] ds_{ij} \quad (31)$$

These coefficients are a solution to a square matrix linear algebraic system defined positive, comprising 12N equations of 12N unknown coefficients a_{kl} for the distribution into five subdomains or 8N equations of 8N unknowns for the division into four subdomains, classically known as Gauss's normal equations:

$$\frac{\partial I(a_{mn})}{\partial a_{kl}} = O \quad (32)$$

The accuracy of the approximate solutions is closely linked to the quality of the alignment of solutions to the auxiliary problems. It is therefore natural to characterize this accuracy by measuring the imperfections of continuity conditions. We will use the assessment of the global error defined in (33) :

$$\eta = \sum_{k<l} \frac{1}{S_{kl}} \int_{\Gamma_{kl}} \left[(u_k - u_l)^2 + \left(\frac{\partial u_k}{\partial \upsilon_k} + \frac{\partial u_l}{\partial \upsilon_l} \right)^2 \right] ds_{kl} \quad (33)$$

where ds_{kl} is the element of the arc length Γ_{ij} , S_{kl} its length and υ_k and υ_l normals to the sub-border Γ_{kl} separating both adjacent subdomains Ω_k an Ω_l.

If the number of coefficients a_{kl} selected increases, the algebraic system to solve gets more and more badly conditioned and the matrix of the system may become numerically singular. The numerical conditioning of an algebraic system is qualified using the number of the spectral conditions of its matrix, known as conditioning.

The conditioning $\chi(A)$ of the square matrix *A* is the product of the Euclidean Norms of *A* and of its inverse A^{-1}

$\chi(A) = \|A\|.\|A^{-1}\|$ [17]

RESULTS AND DISCUSSION

The initial domain (figure 1) comprises eight angular points, among which only four, those with reflex angles measuring $\frac{3\pi}{2}$ are singular for Laplace's equation. At these points where the direction of the normal at the border suddenly changes, they are considered singular. This does not imply that they are automatically analytical singularities. The study of the auxiliary solutions to the auxiliary problems 1 and 5 (equations 21 and 25) shows that at point A, the solution is fully regular since it is defined as well as its partial derivatives of all kinds. At point E,

derivatives $\frac{\partial u_5}{\partial x}$ and $\frac{\partial u_5}{\partial y}$ are finite. A is therefore regular while E is singular. As for our working area, the trapezium ACDE (figure 2), only E is a real singularity. A, C, and D are singular because the normal derivative in these points change direction. B is a "pseudo singularity" introduced to divide up the trapezoid domain. Other divisions of the study area are possible (figure 4). The last two divisions (figure 4c and 4d) allow getting definitely better results as illustrated by the graphs in figures 5 and 6.

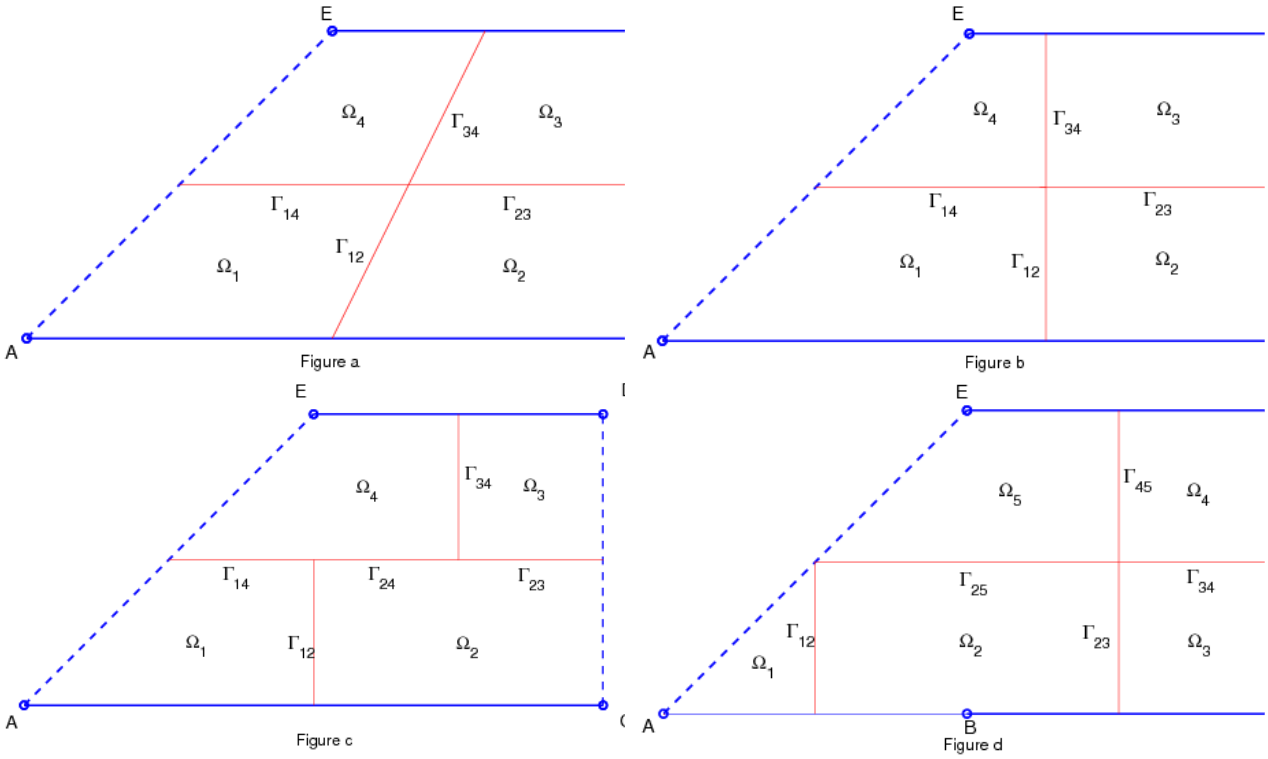

Figure 4 : Various subdivisions of the trapezoid working domain

It is observed that the worst divisions (4a) and (4b) allow getting global errors below 10^{-6} while the division into four subdomains with five subdomains (4c) leads to reduce errors to around 10^{-9} and the division into five subdomains (4d) produces a global error of less than

10^{-12}. Such precision is exceptional for a numerical method and to illustrate the convergence of the method of the large singular finite elements based on the number of coefficients used, we recorded some results in tables 1 and 2. It can be noticed when reading data listed in these tables that the results obtained by using 108 or 144 coefficients are the same to the fourteenth decimal.

Lastly, solving a system of 36 equations to 36 unknowns allows us getting the exact solution near 10^{-8}. We have not got such a precision using the finite elements method, even by solving a system of more than 170,000 equations (figure 13). These results are supported by curves in figure 6 that show the evolution of 10-base logarithm of the conditioning of the matrices of Gauss's various normal equation systems depending on the total number of coefficient kept in the auxiliary solutions 26 to 30. The division (4d) is too flagrant.

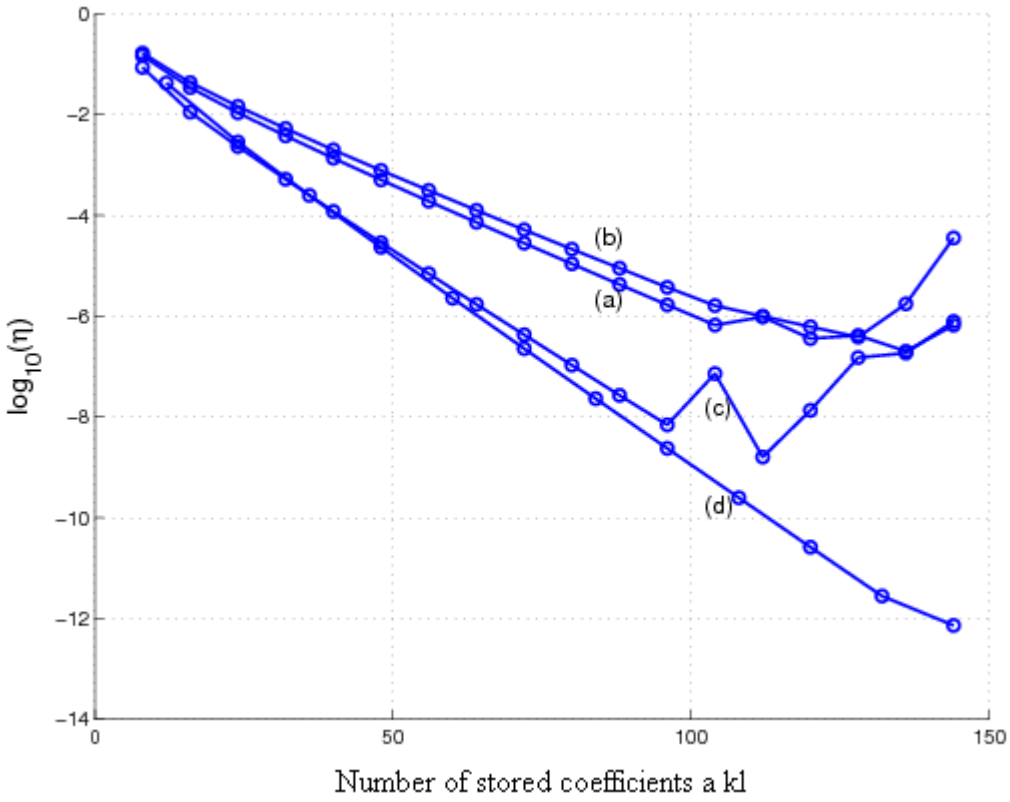

Figure 5: Evolution of the global error according to the number of coefficients a_{kl} kept. Notations (a), (b), (c) and (d) refer to the four subdivisions of the trapezium ACDE (see figure 4)

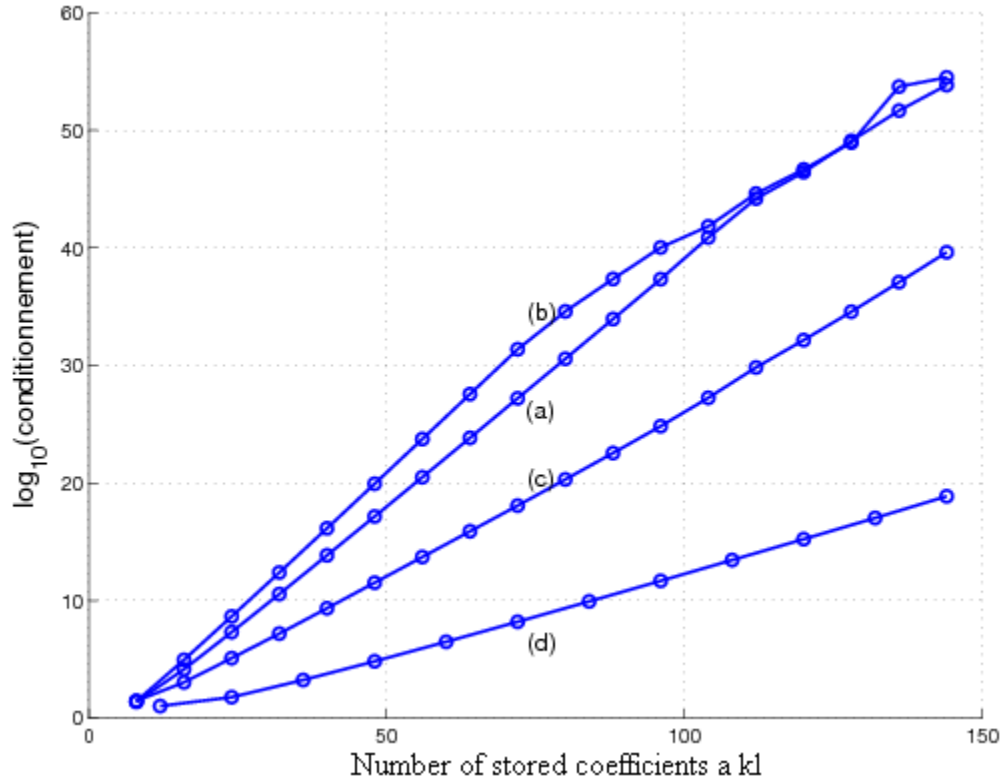

Figure 6 – Conditioning of Gauss's matrix normal equation system
Notations (a), (b), (c) and (d) refer to the four subdivisions of the trapezium ACDE (cf. figure 4).

Table 1: Values of u function near A obtained using LSFEM

$x = y$	36 coefficients	72 coefficients	108 coefficients	144 coefficients
0	0	0	0	0
0.01	0.00007848913159	0.00007848909094	0.00007848909094	0.00007848909094
0.02	0.00031395653117	0.00031395636855	0.00031395636855	0.00031395636855
0.03	0.00070640224195	0.00070640187614	0.00070640187613	0.00070640187613
0.04	0.00125582643197	0.00125582578201	0.00125582578201	0.00125582578201
0.05	0.00196222953814	0.00196222852383	0.00196222852382	0.00196222852382
0.06	0.00282561246788	0.00282561101055	0.00282561101054	0.00282561101054
0.07	0.00384597685845	0.00384597488221	0.00384597488218	0.00384597488218
0.08	0.00502332539383	0.00502332282732	0.00502332282729	0.00502332282729
0.09	0.00635766217944	0.00635765895818	0.00635765895814	0.00635765895814
0.10	0.00784899317449	0.00784898924395	0.00784898924390	0.00784898924390

Table 2: Values of u function near E obtained using LSFEM

$x = y$	36 coefficients	72 coefficients	108 coefficients	144 coefficients
0.90	0.69772520048597	0.69725201311982	0.69725201311831	0.69725201311831
0.91	0.71736439444595	0.71736439826875	0.71736439826736	0.71736439826736
0.92	0.73833264268730	0.73833264655130	0.73833264655002	0.73833264655002
0.93	0.76029077766123	0.76029078144198	0.76029078144081	0.76029078144081
0.94	0.78341911969167	0.78341912328333	0.78341912328228	0.78341912328228
0.95	0.80797111394502	0.80797111725519	0.80797111725426	0.80797111725426
0.96	0.83432477864015	0.83432478158377	0.83432478158297	0.83432478158297
0.97	0.86309440060435	0.86309440309571	0.86309440309505	0.86309440309505
0.98	0.89542367952698	0.89542368146652	0.89542368146601	0.89542368146601
0.99	0.93406930727955	0.93406930852045	0.93406930852014	0.93406930852014
1.00	1.00000000000000	1.00000000000000	1.00000000000000	1.0000000000000

Figure 7 and 8 make think that the potential increases linearly from 0 to 1 along the CD. This is inaccurate as shown in figure 9 where the gap is represented between u and y along CD for 12N=144 and 12N= 96 coefficients kept.

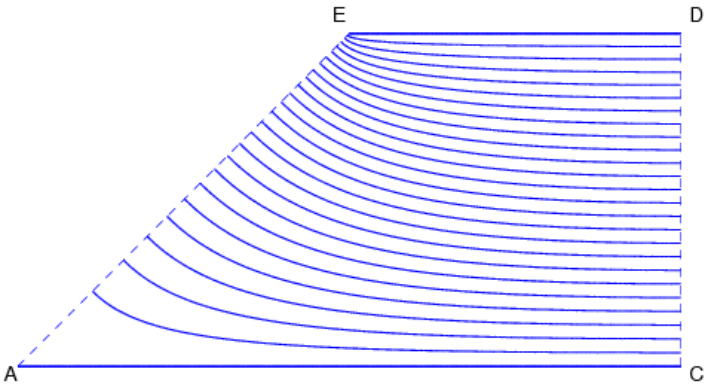

Figure 7- Equipotentials u = (0 : 0.04 :1)

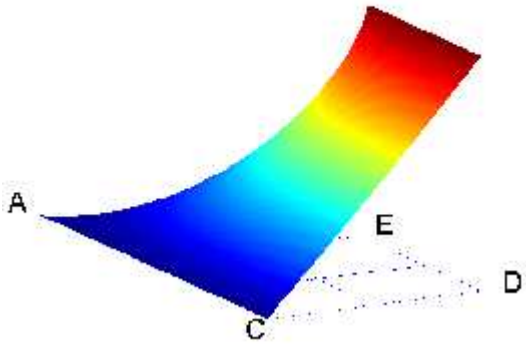

Figure 8- Representation of the function $u(x, y)$ in perspective

The comparison of results obtained using LSFEM and FEM allows us noting that both methods provide results that align quite well all over in the domain Ω, or the trapezium ACDE. Only areas near the singularities is a problem to FEM which encounters difficulties, under its standard form, to provide precise results for derivatives $\frac{\partial u}{\partial x}$ and $\frac{\partial u}{\partial y}$. Graphs 10 and 11 illustrate this good alignment. The first graph gives the values of u along the diagonal AE and the second shows the values of the first partial derivatives $\frac{\partial u}{\partial x}$ (red) and $\frac{\partial u}{\partial y}$ (black) on AE. The abscissa s of diagrams is the length of the arc which goes from 0 to $\sqrt{2}$. Continuous curves are solutions obtained using the large singular finite elements method with 144 parameters while blue circles are values obtained using COMSOL in the case of a grid at a scale of 178,849 degree of freedom.

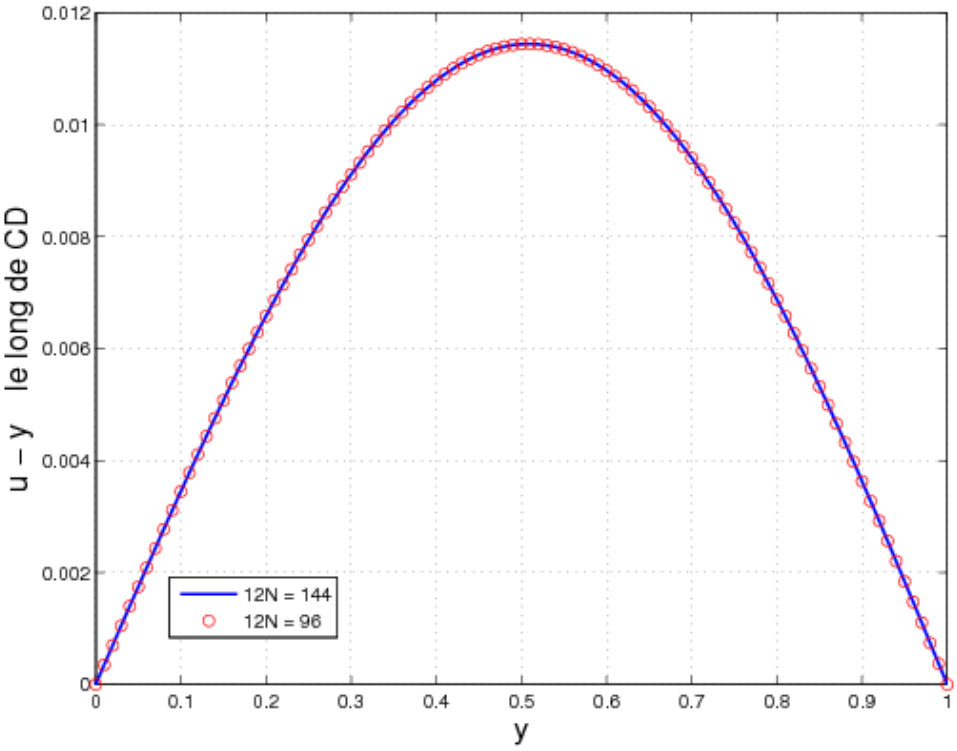

Figure 9- Gap between the function u (x, y) and y along CD

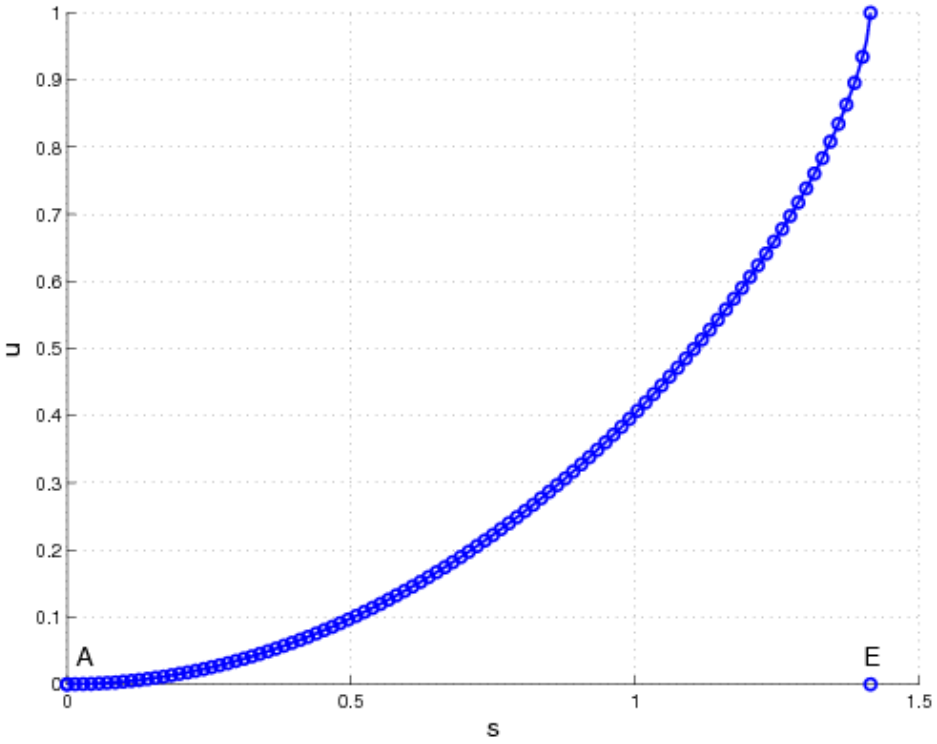

Figure 10 - Potential along AE

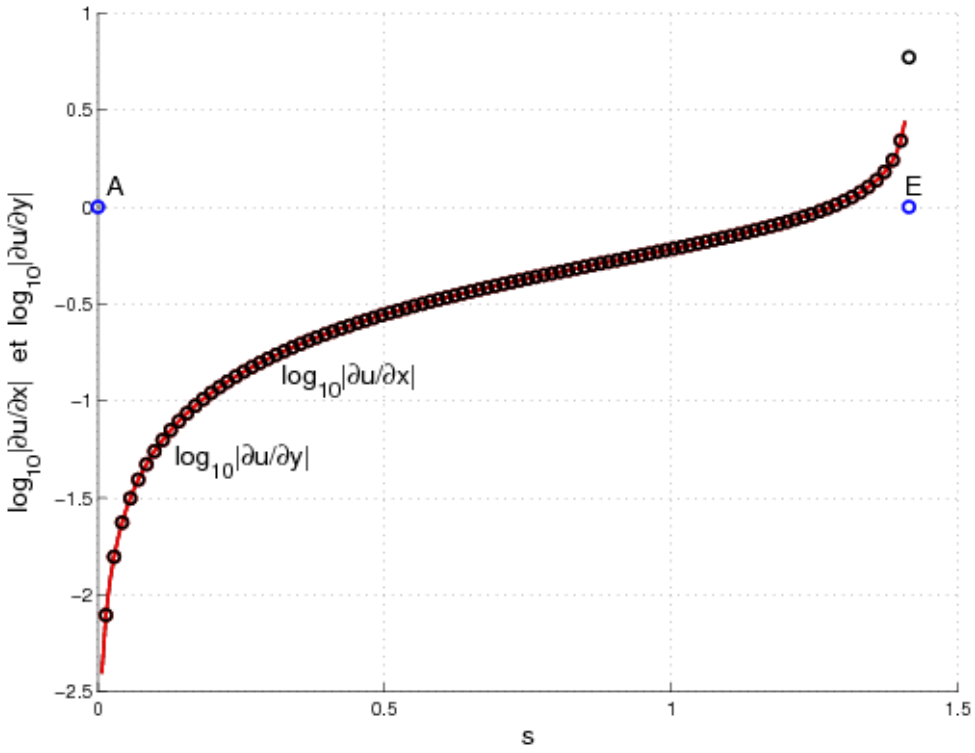

Figure 11- Derivatives of the potential u along AE

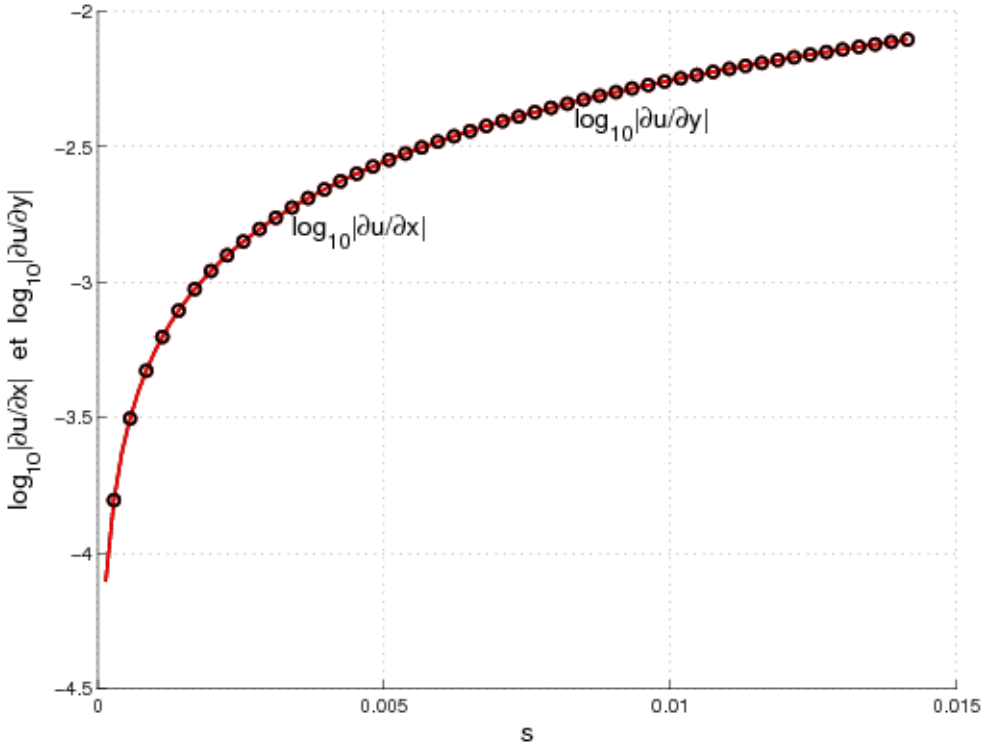

Figure 12 - Derivatives of the potential u along AE, near A

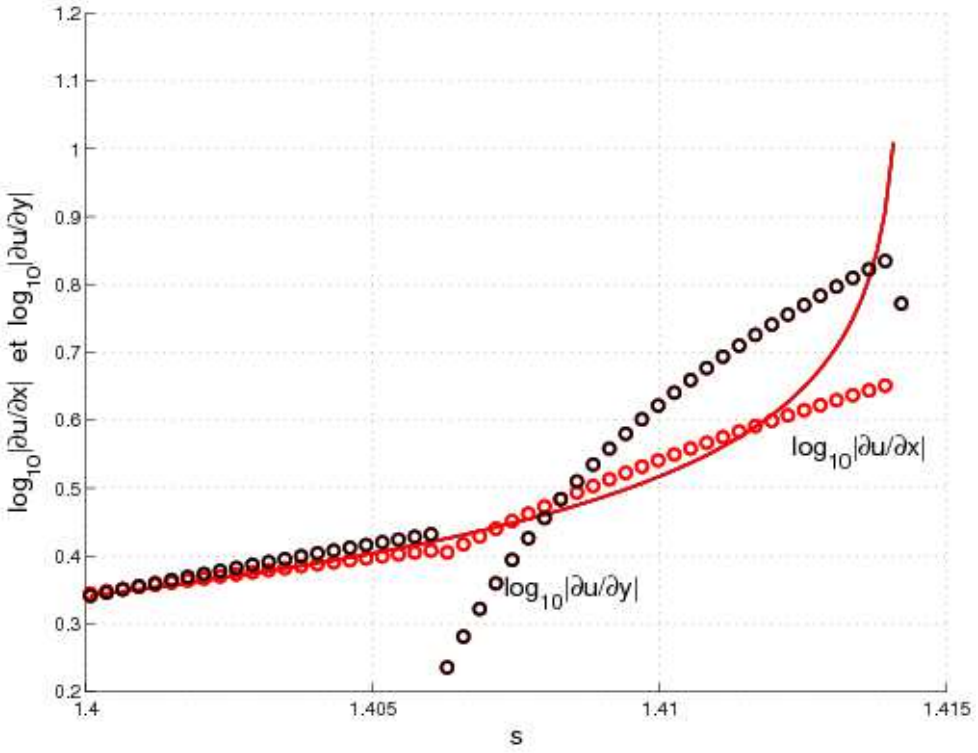

Figure 13- Derivatives of the potential u along AE, near E

The behavior of the approximate solutions near A and E is illustrated in figure 11 where are represented the 10-base logarithms of the modules of derivatives $\frac{\partial u}{\partial x}$ (red) and $\frac{\partial u}{\partial y}$ (black) along the diagonal AE. Continuous curves correspond to values obtained by MGEFS using144 parameters and the circles to those that provide the finite element method using a grid of 178,849 degrees of freedom. Figure 12 gives the same functions near E. we can notice that both methods provide very good results in the area near A, which actually is not a true singularity, while gaps are very significant near singularity E. It should also be noticed that near A, the modules of both partial derivatives merge, which is normal due to the symmetric of the problem. This equality should also be respected near E. Yet, if this is the case for results obtained by LSFEM (red and black curves are merged), it is not the case for those provided by FEM (figure 3).

To complete the comparison between both solving methods, we consider their numerical convergence in some few particular points P_i and we define the relative error by evaluation (35).

$$\varepsilon = 1 - \frac{f_{appx}}{f_{ref}} \tag{35}$$

Where f_{appx} is an approximate value and f_{ref} the reference value. We use the solution obtained by LSFEM while keeping 108 coefficients a_{kl}. Figure 14 shows the evolution of 10-base logarithms of the modules of related errors made and its partial derivatives at each point of the approximate solutions become more and more precise. As abovementioned, blue curves represent the function u, and red ones, the derivative $\frac{\partial u}{\partial x}$ while the black is $\frac{\partial u}{\partial y}$. Circles are related to LSFEM and squares to FEM.

The abscissa scale is the number of parameters a_{kl} kept for LSFEM while for FEM, the five points are representative of approximations provided by the closer and closer grids, leading to an increasing number of degrees of freedom from 2,869 to 178,849. As we may see, results provided by both methods are excellent, especially for the function u. However, the accuracy obtained using LSFEM is considerably better and higher at many extends than that provided by the finite elements method. The gap is at least 8 decades for both u and its derivatives.

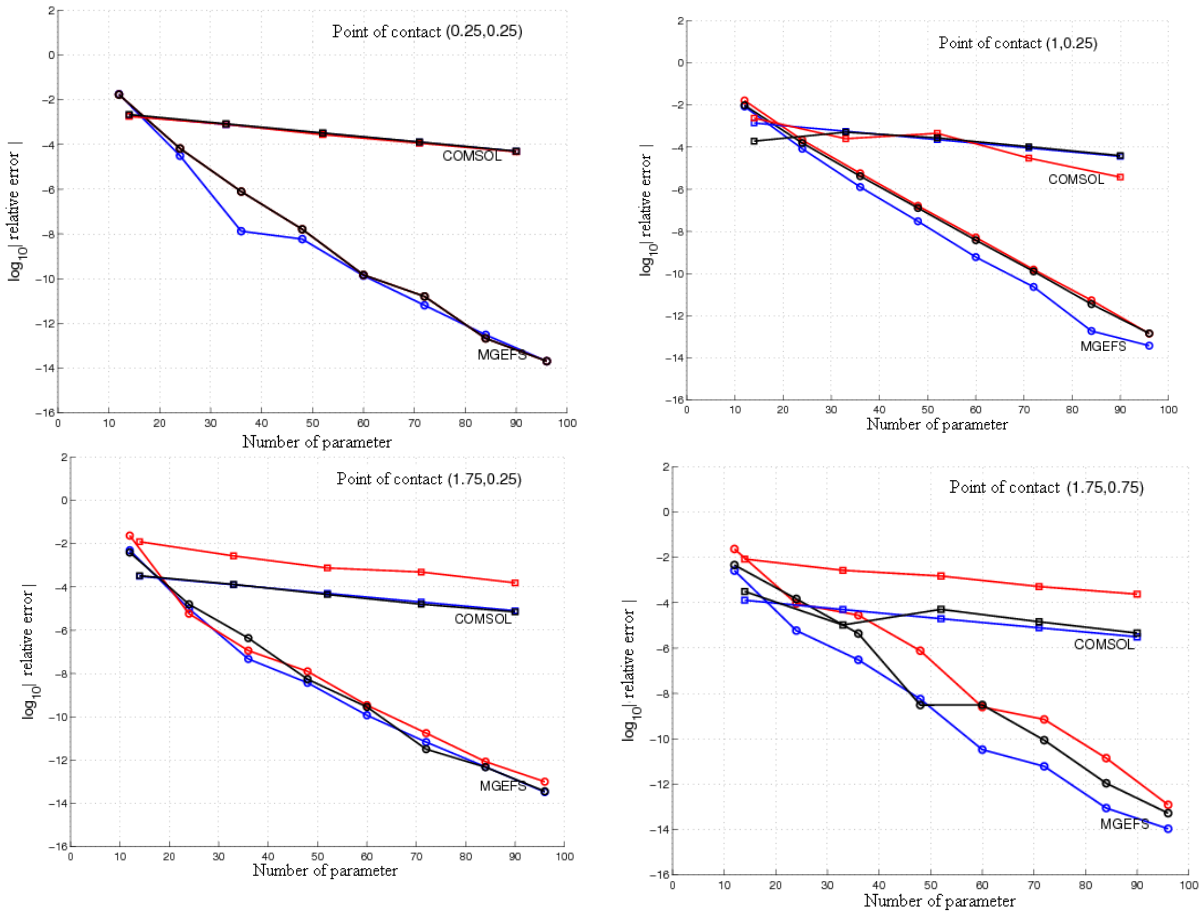

Figure 14- Evolution of related errors on U (blue), $\frac{\partial u}{\partial x}$ (red) and $\frac{\partial u}{\partial y}$ (black)

CONCLUSION

If MGEFS provides good results in the whole study domain, FEM is only satisfactory in areas far from singularities. LSFEM takes into account the existence of singularity to analytically find solution near it, which therefore allows obtaining derivated magnitudes without any additional formulation. The convergence system of the method is exponential. The comparison of results obtained using both methods shows superiority, efficiency, and the accuracy of LSFEM compared to FEM. This study also shows the importance of dividing into subdomains which take symmetries and the number of singularities into account in the method.

Acknowledgements
The authors would like to thank CUD, Belgium, for the grant (CIUF, P2, Physics) and the provision of MATLAB Software to Pr. O. Michel Zongo and Professors M.D. Tolley and B. Haut for receiving them at Université Libre de Bruxelles (ULB).

REFERENCES

[1] O. Maurice, A. Reinex, P. Hoofmann, B. Bernard and P. Pouliguen, *Adv. in Appl. Sci. Res.* **2011**, 2 (5), 439.
[2] V. Sri Hari Babu and G. V. Ramana Reddy, *Adv. in Appl. Sci. Res*. **2011,** 2 (4),138.
[3] D. S. Chauhan and V. Kumar, *Adv. in Appl. Sci. Res*. **2012,** 3 (1), 75.
[4] Z. Yosibash, S. Shannon, M. Dauge, M. Costabel, *Int. J. Fracture*, 2**011**, 168, 31.
[5] O. M. Zongo, S. Kam, S. and A. Ouedraogo, *GJPAS*, **2012**, 18 (1,2), 75.
[6] M. Andrews, *J. Electrostat*. **2006**, 64, 664.
[7] A. F. Emery, *Trans. ASME* (C), **1973**, 95, 344.
[8] O. M. Zongo , PhD Thesis, Université de Ouagadougou, (Ouagadougou, Burkina Faso), **2012.**
[9] M. D. Tolley, PhD Thesis, Université Libre de Bruxelles, (Bruxelles, Belgium), **1977.**
[10] H. Motz, *Quart. Appl. Math*. **1946**, 4, 371.
[11] Z. C. Li and T.T. Lu,. *Math. Comput. Model*. **2000**, 31, 97.

[12] G. Strang and G. Fix, An analysis of the finite element method. Prentice Hall. **1973**.
[13] J. Descloux and M. D. Tolley, *Comput. Method. Appl. Mech. Eng*, **1983**, 39 (1), 37.
[14**]** O. M. Zongo, S. Kam, K. Palm and A. Ouedraogo, *Adv. in Appl. Sci. Res.* **2012**, 3 (3), 1572.
[15] Z. C. Li, T. T. Lu, H.Y. Hu and A. H. D Cheng, *Eng. Anal. Bound. Elem* **. 2005**, 29, 59.
[16] O. M. Zongo, S. Kam, K. Some and A. Ouedraogo, *Adv. in Appl. Sci. Res.* **2013**, 4 (5), 173.
[17] J. Rappaz and M. Picasso, *Analyse numérique*, Presses Polytechniques Romandes, **1998.**